

1 **Increasing persistent hazes in Beijing: potential impacts of weakening East Asian winter**  
2 **monsoons associated with northwestern Pacific sea surface temperature trends**

3  
4 Lin Pei<sup>1\*</sup>, Zhongwei Yan<sup>2</sup>, Zhaobin Sun<sup>1</sup>, Shiguang Miao<sup>1</sup>, Yao Yao<sup>2</sup>

5  
6 <sup>1</sup> Institute of Urban Meteorology, China Meteorological Administration, Beijing, China

7 <sup>2</sup> RCE-TEA, Institute of Atmospheric Physics, University of Chinese Academy of Sciences,

8 Beijing, China

9 \* Corresponding author: lpei@ium.cn

10  
11 **Abstract:**

12 Over the past decades, Beijing, the capital city of China, has encountered increasingly frequent  
13 persistent haze events (PHE). While the increased pollutant emissions are considered as the most  
14 important reason, changes in regional atmospheric circulations associated with large-scale climate  
15 warming also play a role. In this study, we find a significant positive trend of PHE in Beijing for  
16 the winters from 1980–2016 based on updated daily observations. This trend is closely related to  
17 an increasing frequency of extreme anomalous southerly episodes in North China, a weakened  
18 East Asian trough in the mid-troposphere, and a northward shift of the East Asian jet stream in the  
19 upper troposphere. These conditions together depict a weakened EAWM system, which is then  
20 found to be associated with an anomalous warm and high-pressure system in the mid-lower  
21 troposphere over the northwestern Pacific. A practical EAWM index is defined as the seasonal  
22 meridional wind anomaly at 850 hPa in winter over North China. Over the period 1900–2016, this  
23 EAWM index is positively correlated with the sea surface temperature anomalies over the  
24 northwestern Pacific, which indicates a wavy positive trend, with an enhanced positive phase  
25 since the mid-1980s. Our results suggest an observation-based mechanism linking the increase in  
26 PHE in Beijing with large-scale climatic warming through changes in the typical regional  
27 atmospheric circulation.

## 30 1 Introduction

31 In the past decades, pollutant emissions have considerably increased in China because of rapid  
32 economic development (Guo et al., 2011; Zhou et al., 2010). The capital city Beijing encountered  
33 increasingly severe hazes, especially in winter (Niu et al., 2010; Ding and Liu, 2014; Chen and  
34 Wang, 2015; Wang et al., 2015). Notable is the increasing tendency of persistent haze events (PHE)  
35 during the past decades (Zhang et al., 2014; Wu et al., 2017). Severe haze with a high  
36 concentration of fine particles such as  $PM_{2.5}$  not only leads to a sharp decrease in visibility,  
37 causing traffic hazards and disruptions, and, hence, affecting economic activities (Chen and Wang,  
38 2015; Li et al., 2016; Huang et al., 2014), but also induces serious health problems such as  
39 respiratory illnesses, heart disease, premature death and cancers (Pope and Dockery, 2006; Wang  
40 and Mauzerall, 2006; Hou et al., 2012; Sun et al., 2013; Xie et al., 2014; Gao et al., 2015). PHE  
41 would aggravate these serious consequences. From 14–25 January 2013, eastern China was hit by  
42 a severe haze event affecting about 800 million people, while Beijing reached its highest level of  
43 air pollution on record, with the announcement of the first orange haze alert (Sun et al., 2014;  
44 Zhang et al., 2014). In this period, about 200 cases of premature death, and thousands of cases of  
45 hospital admissions for respiratory, cardiovascular and asthma bronchitis diseases were found to  
46 be associated with the high level of  $PM_{2.5}$  (Xu et al., 2013). Correspondingly, this event resulted  
47 in health-related economic losses amounting to about 489 million RMB (~80 million USD). As  
48 both government bodies and the general public have paid extensive attention to the issue of haze,  
49 in particular PHE, detailed studies on the characteristics and the underlying reasons of the  
50 increasing occurrence of PHE around Beijing are urgently needed.

51 Many studies have suggested that the increased emissions of pollutants into the atmosphere  
52 because of rapid economic development and urbanization in China are the main cause of the  
53 increasing number of haze days (Liu and Diamond, 2005; Wang et al., 2013; Wang et al., 2014).  
54 Zhang et al. (2013) suggest that the chemical constituents and sources of  $PM_{2.5}$  in Beijing can  
55 largely vary with season, depending on the meteorology and diverse air-pollution sources. For  
56 pollution in Beijing, vehicles, coal combustion and cross-regional transport are equally important  
57 sources of  $PM_{2.5}$  (He et al., 2013). Nevertheless, specific meteorological conditions play a key role  
58 in forming a haze weather phenomenon (Chen and Wang, 2015; Li et al., 2016; Huang et al., 2014;  
59 Tang et al., 2015; Zhang et al., 2015). The meteorological conditions of the severe haze event in  
60 January 2013 in eastern China were closely related to a weak East Asian winter monsoon (EAWM)  
61 in January, including anomalous southerly flow in the mid-lower troposphere, weakened surface  
62 wind speeds, a reduction of the vertical shear of horizontal winds, and anomalous near-surface  
63 temperature inversion (Zhang et al., 2014). By analyzing the haze episode from 21–26 October  
64 2014, Zhu et al. (2016) found that the severe air pollution in Beijing was formed by southerly  
65 transport and strengthened by local contributions. Conducive meteorological conditions around  
66 Beijing include an inversion in the atmospheric boundary layer, weak wind speeds near the surface,  
67 and sufficient moisture in the air (Liao et al., 2014). Wu et al. (2017) have categorized two types

68 of circulation conditions during PHE in the Beijing–Tianjin–Hebei region: the zonal westerly type  
69 and the high-pressure ridge type, giving rise to descending air in the mid-lower troposphere, thus  
70 leading to a reduced boundary-layer height, with a higher concentration of pollutants near the  
71 surface. While these studies have explored ambient conditions in case studies, the large-scale  
72 atmospheric circulation background of PHE around Beijing remains unclear from the perspective  
73 of long-term climate change.

74 Recently, the role of underlying climatic factors in modulating regional weather conditions in  
75 association with severe haze events has been reported, and is expected to have influenced the  
76 change in the severity of hazes (e.g., Niu et al., 2010; Wang et al., 2015; Cai et al., 2017; Zou et al.,  
77 2017; Yin and Wang, 2017). These climatic factors include a weakened EAWM system and the  
78 associated decreased near-surface wind speeds (Niu et al., 2010) and increased relative humidity  
79 in the region (Chen and Wang, 2015), reduced Arctic sea ice (Wang et al., 2015), and anomalous  
80 sea surface temperature (SST) in the subtropical western Pacific (Yin and Wang, 2016). The  
81 observed negative trend of the EAWM during the past few decades caused significantly reduced  
82 wind speeds over North China, subdued atmospheric transport of pollutants, and hence contributed  
83 to the increasing number of haze days (Niu et al., 2010; Huang et al., 2012; Li et al., 2016). The  
84 latest studies have analyzed the possible influences of anthropogenic climate change on haze  
85 occurrences (e.g. Cai et al., 2017; Zou et al., 2017; Yin and Wang, 2017). Based on historical and  
86 future climate simulations, Cai et al. (2017) suggested that anthropogenic greenhouse gas  
87 emissions and the associated changes would increase the occurrences of weather conditions  
88 conducive to Beijing winter severe haze. Zou et al. (2017) indicated that the unprecedented severe  
89 haze event in January 2013 resulted from the extremely poor ventilation conditions in eastern  
90 China, which is linked to Arctic sea ice loss and extensive Eurasian snowfall. However, the  
91 connection of the underlying climatic factors to the changes in PHE around Beijing remains  
92 unclear, especially on long-term (multidecadal to centennial) timescales, and, specifically, the  
93 extent to which large-scale climate change may have contributed to the local pollution changes in  
94 Beijing in the last decades.

95 In this paper, we investigate the climatology of PHE in Beijing for the winter monsoon season  
96 including long-term changes in PHE connected with large-scale climate change. First, based on  
97 updated daily observations, we examine the increase in PHE in Beijing from 1980 to 2016. We  
98 then analyze the associated changes in atmospheric circulation, especially those connected with  
99 the EAWM, and explore a relationship between the EAWM and sea surface temperature anomalies  
100 (SSTA) over the northwestern Pacific for the centennial period 1900–2016. Finally, we propose a  
101 mechanism linking the large-scale climate warming, the weakening EAWM and the positive trend  
102 of PHE in Beijing. We describe the data and methods used in Sect. 2, and demonstrate the changes  
103 of PHE in Beijing in the past decades, the associated changes of climatic conditions related to the  
104 EAWM system, and the connection between the EAWM and SSTA over the northwestern Pacific  
105 since 1900 in Sect. 3, with a discussion and summary given in Sect. 4.

## 106 2 Data and methods

### 107 2.1 Definition of a haze day,

108 Haze is a multidisciplinary weather phenomenon defined by different variables depending on the  
109 branch, e.g., visibility and humidity in meteorology, and  $PM_{2.5}$  concentration in the environmental  
110 sciences. In meteorology, haze is usually defined based on the observations of relative humidity  
111 and visibility with specified criteria depending on the organization (e.g., the World Meteorological  
112 Organization and the UK Met Office) or the empirical analyses (e.g., Schichtel et al., 2001; Doyle  
113 and Dorling, 2002; Wu, 2006; Vautard et al., 2009; Ding and Liu, 2014). In China, the standard  
114 observational procedures and criteria of a weather phenomenon record of ‘haze’ were not unified  
115 until around 2000, so that the weather phenomenon observation record cannot be directly used in  
116 climate research (Wu et al., 2009). In contrast, the observations of visibility and humidity were  
117 quite evenly distributed over a longer temporal range, which enables the establishment of  
118 long-term time series of haze. In general, a haze day should be of a weather phenomenon record of  
119 ‘haze’ with visibility < 10 km and relative humidity < 90%. There were mainly three methods for  
120 defining a haze day, which are based on these criteria with any single observation beyond the  
121 criteria in the day, the daily mean and the observation at 14:00PM, respectively. Wu et al. (2014)  
122 have suggested that the calculation based on the daily mean criteria involves more widespread and  
123 lasting haze processes, while that based on records at 14:00PM neglects haze events with poor  
124 visibility caused by the rise in humidity in the morning and night. Therefore, in this study, a haze  
125 day is defined if a haze weather phenomenon is recorded with daily mean visibility < 10 km, and  
126 daily mean relative humidity < 90%. Persistent haze events are defined here as haze events  
127 recorded at more than one site in the region for four consecutive days in Beijing. The number of  
128 persistent haze days is calculated as the sum of the days during a particular event.

129 The meteorological data used here are from the quality-controlled station observations collected at  
130 the National Meteorological Information Center of China, including the relative humidity,  
131 visibility, and weather phenomenon records. The data include four observations per day at 02:00,  
132 08:00, 14:00, and 20:00 local time (LT). Consecutive records during the winters (December,  
133 January and February, DJF) from 1980 to 2016 at 20 stations in Beijing are used. For example, the  
134 winter of 1980 refers to the average of December 1980, January 1981 and February 1981. The  
135 visibility data at stations were obtained in different ways before and after 2013. Before 23 January  
136 2013, the visibility was measured for meteorological purposes as a quantity estimated by a human  
137 observer. Since then, the observations of visibility have been transformed to instrumental  
138 measurements of the meteorological optical range (MOR). MOR is defined as the length of the  
139 path in the atmosphere required to reduce the luminous flux of a collimated beam from an  
140 incandescent lamp at a color temperature of 2700 K to 5 percent of its original value; the luminous  
141 flux is evaluated by means of the photometric luminosity function of the International  
142 Commission on Illumination (WMO, 2008). According to the theoretical calculation (WMO, 1990;

143 2008), the transformation formula between the visual estimate  $VIS_{Observer}$  and the instrumental  
144 measurement  $VIS_{Instrumental}$  is

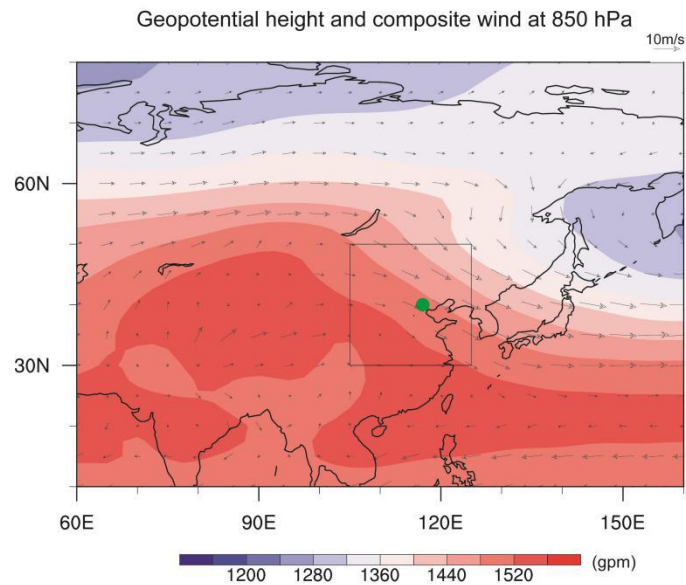
$$145 \quad \frac{VIS_{Instrumental}}{VIS_{Observer}} = \frac{(1/\kappa) \times \ln(1/0.05)}{(1/\kappa) \times \ln(1/0.02)} \approx 0.766, \quad (1)$$

146 where  $\kappa$  is the extinction coefficient. As it is necessary to adjust these data and maintain their  
147 consistency before analysis, the visibility observations from 2013–2016 are transformed to be  
148 comparable with the earlier visual estimations.

## 149 **2.2 Global climate observations**

150 The daily and monthly data of wind speed, geopotential height, specific humidity, sea level  
151 pressure and air temperature from the NCEP/NCAR (National Centers for Environmental  
152 Prediction/National Center for Atmospheric Research) for the period of 1980–2017 at 2.5°  
153 resolution (Kalnay et al., 1997) are used for the analysis of atmospheric conditions during PHE.  
154 We also use the monthly data of meridional wind at 850 hPa for the period 1900–2010 from the  
155 20th Century Reanalysis (20CR) version 2 at 2° resolution (Compo et al., 2011), and the European  
156 Centre for Medium-Range Weather Forecasts Atmospheric Reanalysis (ECMWF) of the 20th  
157 Century (ERA-20C) at 1° grid resolution (Poli et al., 2016). The monthly SST data used are from  
158 the Hadley Center Sea Ice and Sea Surface Temperature (HadISST) dataset version 1.1 at 1°  
159 resolution (Rayner et al., 2003) for the period 1900–2016.

160 The dominant feature of the winter monsoon over East Asia is the northwesterly wind direction in  
161 the lower troposphere (Fig. 1). During severe haze, northwesterly flow from the near-surface to  
162 mid-lower troposphere weakens, or even reverses to a southerly direction, indicating a weak  
163 EAWM system (Niu et al., 2010). The daily meridional wind anomaly at 850 hPa over eastern  
164 China was found to be critical to the accumulation of  $PM_{2.5}$  in Beijing (Cai et al., 2017). Here, we  
165 define a practical index for assessing the EAWM strength as the seasonal mean meridional wind  
166 anomaly at 850 hPa during winter over the region (30°–50°N, 105°–125°E) as outlined in Fig. 1.  
167 This seasonal anomaly ( $I_w$ ) is calculated with respect to the climatological mean level ( $I_{wmean}$ )  
168 from 1981 to 2010. An extreme anomalous southerly day is so defined if the daily meridional  
169 wind anomaly exceeds  $2\sigma$  (the standard deviation of the  $I_w$  series) beyond  $I_{wmean}$ , representing  
170 an unusually weak winter monsoon weather condition.



171

172 **Fig. 1. Climatological mean of geopotential height (shading, units: gpm) and composite wind**  
 173 **speed (vectors) at 850 hPa in winter over East Asia during 1980–2016. The outlined region**  
 174 **(30 °–50 ° N, 105 °–125 ° E) is used to calculate a regional mean climatological background**  
 175 **around Beijing (green dot, 40 °N, 117 °E).**

### 176 2.3 Ensemble Empirical Mode Decomposition

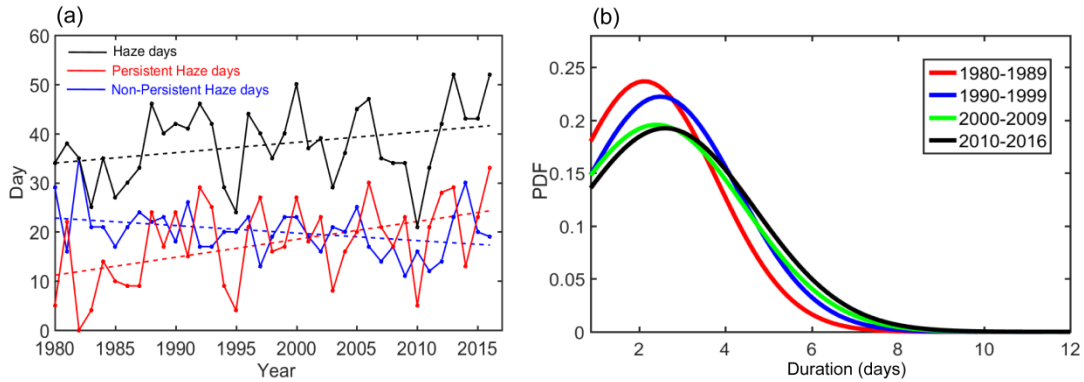
177 In this study, the ensemble empirical mode decomposition (EEMD) method is applied to separate  
 178 the multidecadal-to-centennial timescale variations of SSTA time series over the northwestern  
 179 Pacific. The EEMD method is an adaptive time–frequency, data analysis technique developed by  
 180 Wu et al. (2007) and Wu and Huang (2009). It is an efficient way to separate specific timescale  
 181 variations in the original data series. The EEMD method is a refinement of the empirical mode  
 182 decomposition (EMD) method, which emphasizes the adaptiveness and temporal locality of the  
 183 data decomposition (Huang et al. 1998; Huang and Wu 2008). With the EMD method, any  
 184 complicated data series can be decomposed into a few amplitude–frequency-modulated oscillatory  
 185 components called intrinsic mode functions (IMF) at distinct timescales.

186 The main steps of the EEMD analysis are as follows (Qian, 2010): (1) add a random white noise  
 187 series with an amplitude of 0.2 times the standard deviation of the data to the target time series to  
 188 provide a relatively uniform and high-frequency extreme distribution, allowing the EMD method  
 189 to avoid the effect of potential intermittent noise in the original data; (2) decompose the data with  
 190 the added white noise into IMFs using the EMD method; (3) repeat steps 1–2 for 1000 times, but  
 191 with distinct random white noise series added each time; (4) obtain the mean IMF of the 1000  
 192 ensemble results to produce the final result.

193 With the EEMD method, the SSTA series over the northwestern Pacific ( $120^{\circ}\text{--}150^{\circ}\text{E}$ ,  $26^{\circ}\text{--}40^{\circ}\text{E}$ )  
 194 in winter during 1900–2009 is decomposed into a nonlinear secular trend and five major  
 195 timescales of IMF (figure not shown). The multidecadal variability is represented by the fifth IMF,  
 196 with an oscillatory period between half and one century.

### 197 3 Results

#### 198 3.1 Increasing persistent haze events in Beijing from 1980 to 2016



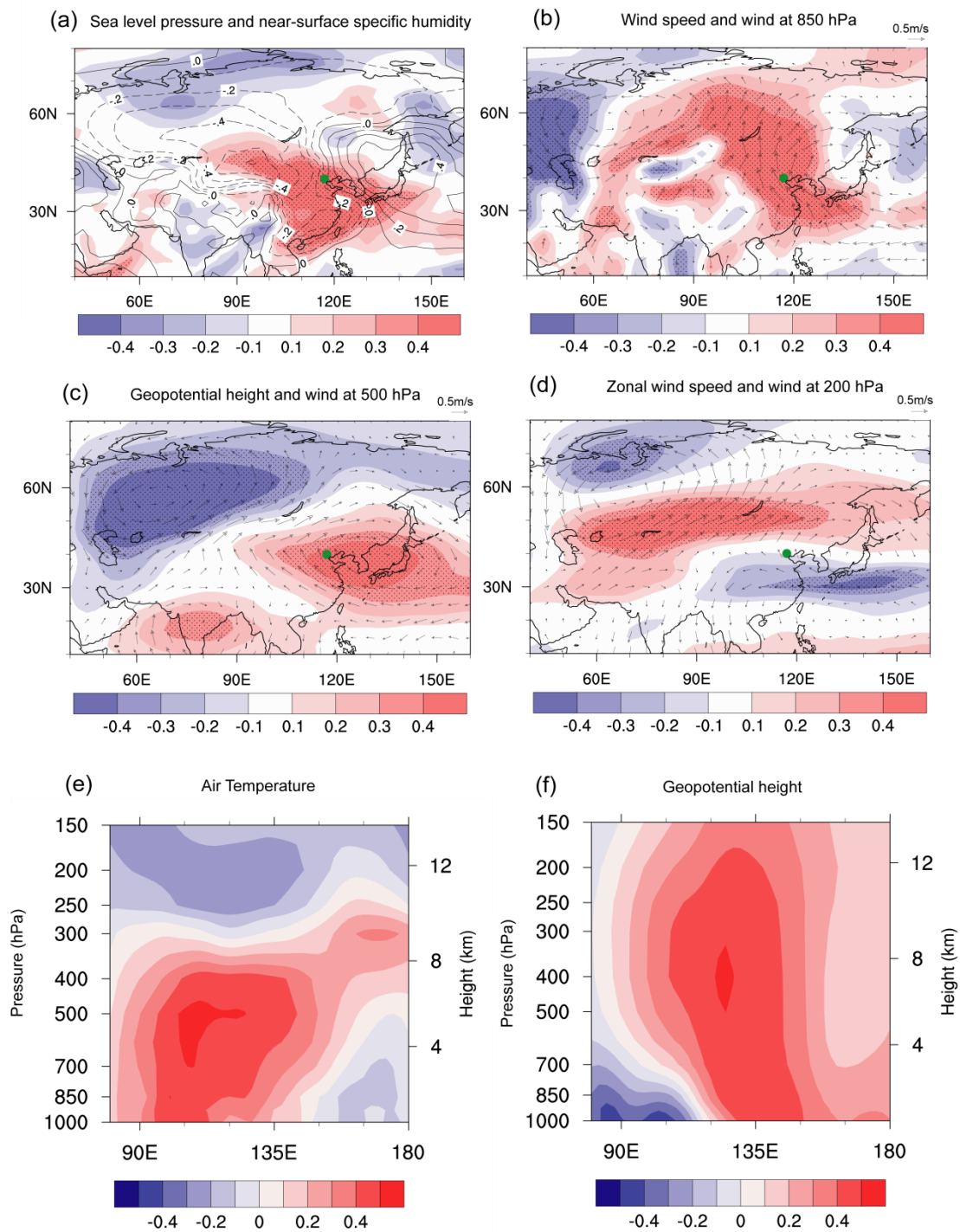
199

200 **Fig. 2. (a) Number of haze days (black), persistent haze days (red) and non-persistent haze**  
 201 **days (blue) in winter in Beijing from 1980 to 2016. Dashed lines show the least-squares**  
 202 **trends. (b) Probability distribution function (PDF) of the duration (days) of haze events in**  
 203 **Beijing for each decadal period from 1980 to 2016.**

204 The number of haze days in Beijing exhibits a large inter-annual variability with a non-significant  
 205 positive trend (black curve in Fig. 2a) consistent with previous studies (e.g., Chen and Wang,  
 206 2015). However, the number of persistent haze days (red curve) in Beijing exhibits a significant  
 207 positive trend, while that of the non-persistent haze days (blue curve) exhibits a significant  
 208 negative trend, both at the 0.05 level. Figure 2b shows the duration of haze events in Beijing have  
 209 changed in this period, with most haze events lasting for about 3 days. The largest shift in the  
 210 maximum of the PDF occurred from the 1980s to the 1990s, with a higher probability of events  
 211 with durations longer than 3 days. Since then, the maximum of the PDF has decreased with  
 212 increasing probability of persistent haze events longer than 4 days. These results show that it is the  
 213 number of persistent haze days that has been increasing from 1980 to 2016 and the duration of  
 214 haze events tends to get longer over the last decades.

215

#### 216 3.2 Meteorological conditions for persistent haze events



217

218 **Fig. 3.** The correlation coefficients between the number of persistent haze days and (a)  
 219 specific humidity at 1000 hPa (shading) and sea level pressure (contour); (b) composite wind  
 220 speed (shading) and in addition the composite wind (vectors) at 850 hPa; (c) geopotential  
 221 height (shading) and in addition the composite wind (vectors) at 500 hPa; (d) zonal wind  
 222 speed (shading) and in addition the composite wind (vectors) at 200 hPa; (e) vertical profile  
 223 of air temperature at 40°N; and (f) vertical profile of geopotential height at 40°N in winter

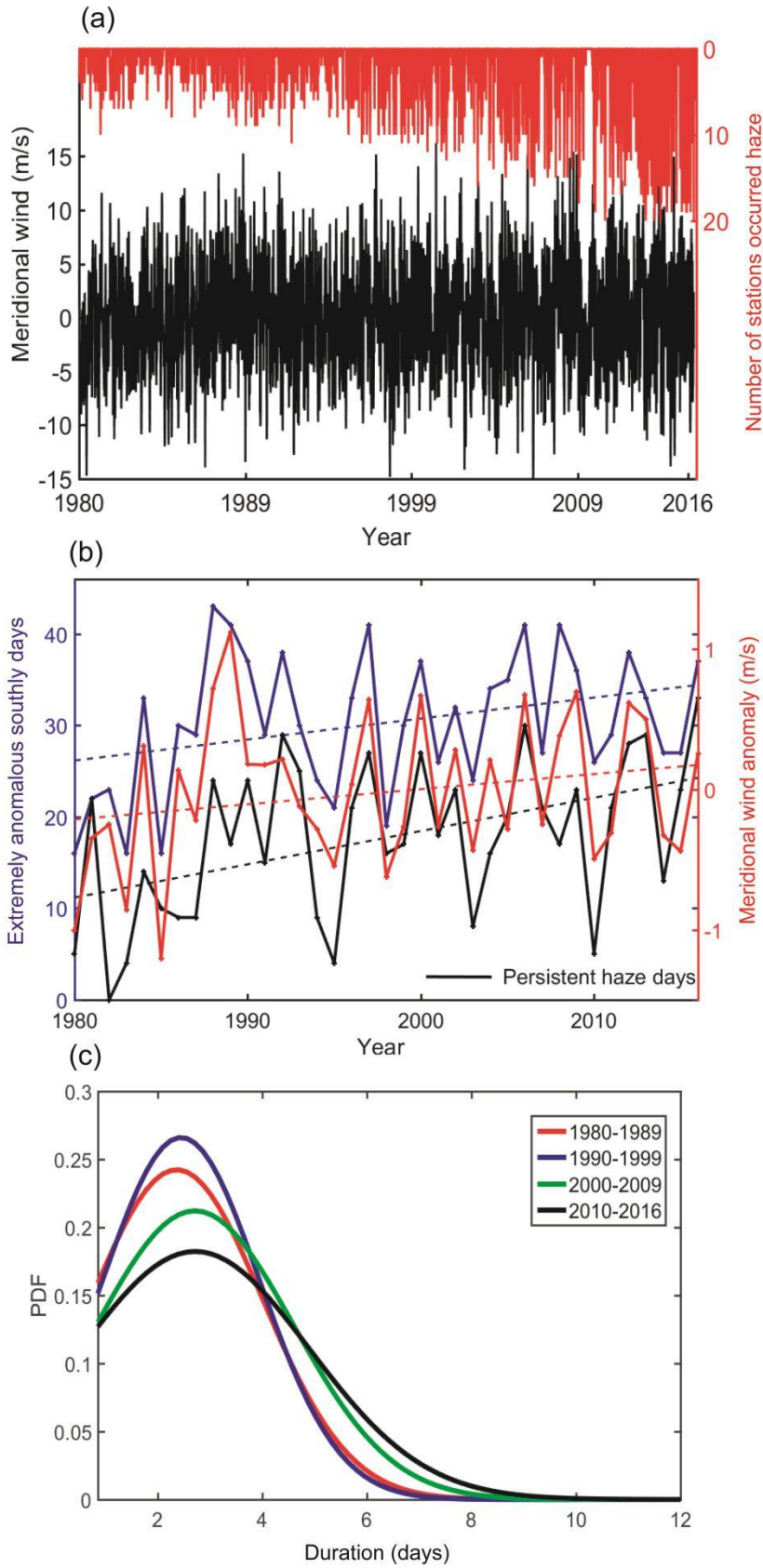


224 **from 1980 to 2016 based on the monthly NCEP/NCAR reanalysis data. The linear trend is**  
225 **removed before calculating the correlation. The black dots indicate significant changes at the**  
226 **0.05 level using the t-test. The green dot denotes the location of Beijing (40 °N, 117 °E).**

227 Figure 3 depicts correlation coefficients between anomalous variables of atmospheric circulation  
228 from the near-surface to upper troposphere, and the number of persistent haze days in Beijing in  
229 winter from 1980–2016. In the lower troposphere (Fig. 3a), most of China is covered by an  
230 anomalous low-pressure system adjacent to an anomalous high over the northwestern Pacific,  
231 suggesting weaker-than-usual northerly winds from the mid-high latitudes. Consequently, North  
232 China is covered by widespread anomalous southerlies, implying significant weakening of the  
233 northerly winds, or even reversal to a southerly flow in the region (Fig. 3b). The southerly  
234 anomalies over eastern China are favorable for the transport of warm, moist air from the southern  
235 to the northern part of eastern China, creating favorable humidity conditions for the occurrence of  
236 haze (Fig. 3a). At 500 hPa, East Asia is mainly dominated by an anomalous high (Fig. 3c),  
237 representing a shallow East Asian trough. The associated northwesterly wind exists to the north  
238 rather than the south of Beijing, limiting the cold and dry northwesterly flow to Beijing, as well as  
239 reducing wind speeds in Beijing, unfavorable for the clearance of pollutant. At the upper  
240 troposphere at 200 hPa, the East Asian jet stream shifts northwards (Fig. 3d) with enhanced zonal  
241 circulation in the high latitudes (north of 45 °N) and weakened meridional circulation over East  
242 Asia. This pattern indicates weak cold-air activities around Beijing. The decreased zonal wind  
243 speed in the middle latitudes favors the maintenance and enhancement of the pollutant  
244 convergence needed for the occurrence of haze. The weakened EAWM system (e.g. Niu et al.,  
245 2010; Wang and He, 2013; Chen and Wang, 2015) was responsible for these changes favorable for  
246 the formation of PHE in Beijing. As shown in Fig. 3e and f, a system with an anomalously warm  
247 temperature and high geopotential height from 850 hPa to 300 hPa is located over the  
248 northwestern Pacific (40 °N, 120 °–150 °E). The anomalous warm air in the mid-lower troposphere  
249 facilitates a crucial thermodynamic mechanism limiting the vertical transport of aerosol particles  
250 within the boundary layer because of increased stability, which is favorable for the trapping of  
251 pollution and moisture in the atmospheric boundary layer in the region around Beijing. Such an  
252 anomalous vertical structure also causes descending motion in the mid-lower troposphere, giving  
253 rise to a reduction in the height of the atmospheric boundary layer, and enhancement of the  
254 pollutant convergence in the region. In short, all of these related atmospheric circulation anomalies  
255 are favorable for the maintenance and development of PHE in Beijing.

256

257 **3.3 Variations of meridional wind anomaly at 850 hPa and the relationship with persistent**  
258 **haze events**



259

260 **Fig. 4. (a) Number of stations where haze is recorded in Beijing (red) versus daily meridional**

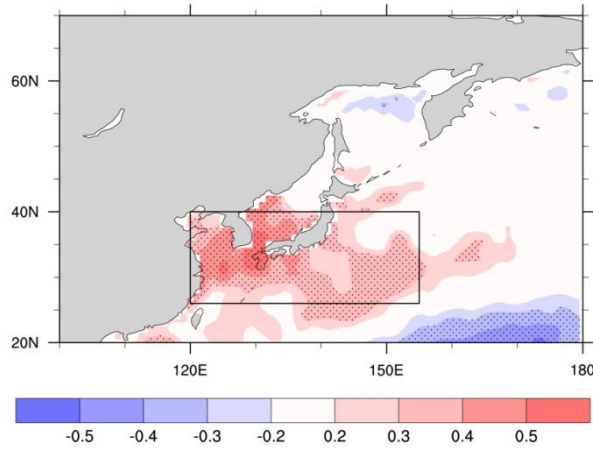
261 **wind at 850 hPa over the study region (30 °–50 ° N, 105 °–125 ° E) (black) in winter from**  
262 **1980–2016. (b) Meridional wind anomaly (red), number of extremely anomalous southerly**  
263 **days (blue) and persistent haze days (black) in winter from 1980–2016. Dashed lines show**  
264 **the least-squares trends. (c) The PDF of the duration (days) of extremely anomalous**  
265 **southerly episodes for each decade from 1980–2016.**

266 A weakening EAWM system is anticipated regarding the changes of meteorological conditions in  
267 Fig. 3 as partly discussed in previous studies (e.g., Niu et al., 2010; He et al., 2013; Wang and He,  
268 2013; Yin and Wang, 2016). During PHE, the northerly winter monsoon weakens and brings less  
269 cold, dry air to the region, which is favorable for both the formation and maintenance of PHE.  
270 According to our analysis, meridional wind anomaly at 850 hPa in North China may be one of the  
271 most effective meteorological conditions for the occurrence of PHE.

272 As shown in Fig. 4a, the daily meridional wind anomaly is notably correlated with the number of  
273 haze stations in winter during 1980–2016, with a correlation coefficient of 0.43 significant at the  
274  $\alpha = 0.01$  level. It suggests the strong likelihood of haze in Beijing during anomalous southerlies in  
275 North China. The seasonal meridional wind anomaly series in winter exhibits a strong interannual  
276 variability with a non-significant positive trend (red lines in Fig. 4b). However, the number of  
277 extremely anomalous southerly days exhibits a significant positive trend (at the 0.05 level) and a  
278 significant positive correlation coefficient of 0.70 with the number of persistent haze days in  
279 Beijing. This coefficient remains as large as 0.66 between the de-trended series, and is significant  
280 at the  $\alpha = 0.01$  level. As shown in Fig. 4c, the duration of extreme anomalous southerly events has  
281 changed in the recent decades, with most of these events lasting for 2–3 days. From the 1980s to  
282 the 1990s, the maximum of the wind PDF increases with more 3–4-day events, but without much  
283 change toward the longer duration end, indicating mainly an increasing probability of extreme  
284 southerly events lasting for 2–4 days. Since then, the maximum of the PDF has been decreasing  
285 with increasing probability of extreme southerly episodes of longer duration. In comparison with  
286 Fig. 2b, the changes in the PDF of the anomalous southerly wind episodes mostly explain the  
287 occurrence of PHE in Beijing over the period from 1980–2016. However, the relationship between  
288 the two is not simply linear. The striking shift of the PDF of haze events from the 1980s to the  
289 1990s is notable, indicating a rapid increasing probability of longer duration haze events, with the  
290 rapid increase of pollution in the region during the 1990s likely responsible. As pointed out by  
291 Guo et al. (2011), there was a significant increase of the aerosol optical depth from 1980 to the  
292 1990s in most of China, especially in North China, corresponding to a rapid development of both  
293 urbanization and industrial activities in the region in that time.

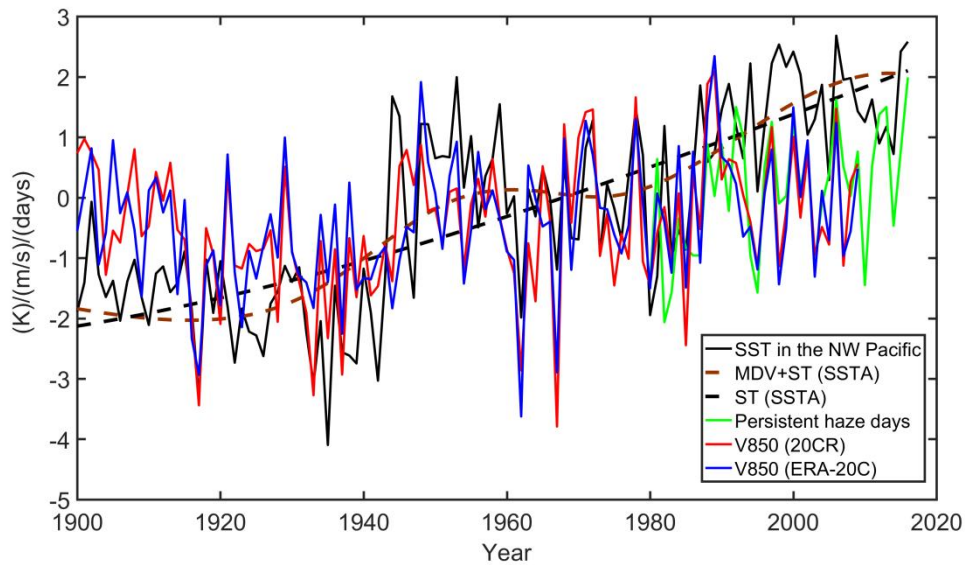
294

295 **3.4 Connections between the meridional wind anomaly and sea surface temperature**  
296 **anomaly over the northwestern Pacific since 1900**



297

298 **Fig. 5. The correlation coefficients between the SSTA in the northwestern Pacific and the**  
299 **number of extreme anomalous southerly days in winter in North China from 1980–2016. The**  
300 **linear trend is removed before calculating the correlation. The black dots indicate a**  
301 **significant correlation at the 90% confidence level using the t-test.**



302

303 **Fig. 6. Time series of the normalized SSTA in the northwestern Pacific (black), meridional**  
304 **wind anomaly at 850 hPa in North China from the 20CR (red) and ERA-20C (blue) datasets,**  
305 **and persistent haze days (green) from 1900–2016. The climatic mean is calculated for the**

306 **period 1961–1990. The black dotted curve is the secular trend (ST) of SSTA series; the**  
307 **brown dotted curve is the combination of the secular trend and the multidecadal variability**  
308 **(MDV) of SSTA series, obtained via the EEMD method.**

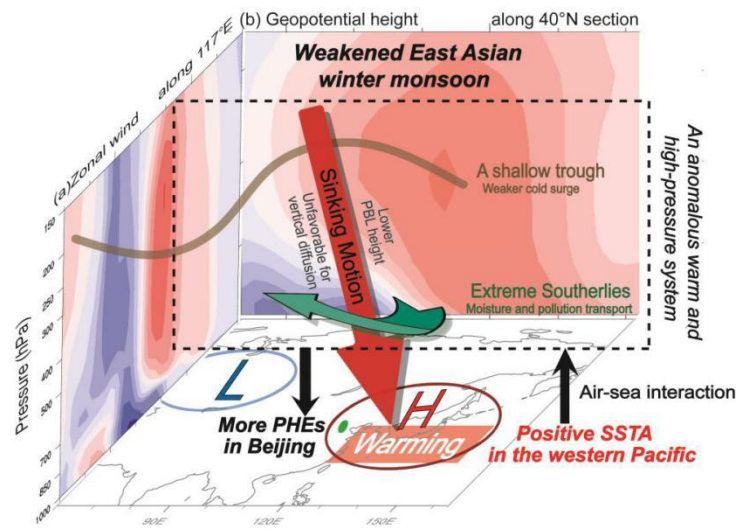
309 As shown in Fig. 5, there is a positive correlation zone in the subtropical to mid-latitude  
310 northwestern Pacific (120 °–155 °E, 26 °–40 °E), suggesting that northerly winter monsoons in East  
311 Asia become weaker with more extreme anomalous southerly episodes when the subtropical  
312 northwestern Pacific is warmer. It is interesting to investigate this relationship over a longer period.  
313 As shown in Fig. 6, over the past centennial period 1900–2016, the SSTA in the subtropical  
314 northwestern Pacific and the meridional wind anomalies at 850 hPa over North China are well  
315 correlated, especially at a multidecadal timescale. The correlation coefficients are 0.46 (detrended:  
316 0.42) and 0.51 (detrended: 0.53) based on the ERA-20C and 20CR datasets for the period  
317 1900–2009, respectively, and significant at  $\alpha = 0.01$ . The results here are generally consistent with  
318 the physical mechanism simulated by Sun et al., (2016), which demonstrates the role of the  
319 northwestern Pacific SST on the EAWM. Furthermore, the correlation coefficient between  
320 normalized persistent haze days and normalized SSTA series for the period 1980–2016 is 0.41,  
321 significant at  $\alpha = 0.01$ . Thus, the linkages between persistent haze days, anomalous southerly  
322 episodes and SSTA over the northwestern Pacific are significant, even over the past centennial  
323 period for 1900–2016. From 1900–2016, the regional mean SSTA over the northwestern Pacific  
324 showed a non-linear secular positive trend. The combination of multidecadal variability and the  
325 secular trend of SSTA exhibit a sharp positive phase since the mid-1980s. As discussed above, the  
326 notable warming phase since the mid-1980s over the NW Pacific should correspond to a  
327 weakened EAWM system, in particular with increasing extreme anomalous southerly episodes,  
328 hence increasing PHEs in Beijing.

329

#### 330 **4. Discussion and Summary**

331 Here we investigate the climatology of PHE in Beijing for the winter monsoon season and explore  
332 the potential impacts of large-scale climate change on the positive trend of PHE. Based on updated  
333 daily observations, we have demonstrated the variations of haze days in winter with a significant  
334 increasing frequency of PHE in Beijing from 1980–2016. The associated changes in large-scale  
335 atmospheric circulation include weakened near-surface northerly winds in North China, a shallow

336 East Asian trough in the mid-troposphere, and a northward shift of the East Asia jet stream in the  
 337 upper troposphere. These conditions indicate a weakened EAWM system, which was then found  
 338 to be associated with an anomalous warm, high-pressure system in the mid-lower troposphere over  
 339 the northwestern Pacific. One of the most direct factors for the occurrence of PHE in Beijing is the  
 340 persistent anomalous southerlies in the lower troposphere in North China. From 1980 to 2016,  
 341 changes of the regional extreme anomalous southerlies correspond well to those of the persistent  
 342 hazes in Beijing. Therefore, the increasing frequency of longer-duration anomalous southerly  
 343 episodes in the past decades explains the increasing occurrences of PHE in Beijing. Furthermore,  
 344 we find that even for the past centennial period 1900–2012, the meridional wind anomaly at 850  
 345 hPa in North China is positively correlated with the SSTA over the northwestern Pacific.



346  
 347 **Fig. 7. Schematic diagram summarizing the dynamic connection between the increased**  
 348 **SSTA in the northwestern Pacific and the increasing PHE in Beijing through the weakening**  
 349 **East Asian winter monsoon system. The cross sections are correlation coefficients between**  
 350 **the meridional wind-speed anomaly and vertical profile of (a) zonal wind speed at 117° E**  
 351 **and (b) geopotential height at 40° N and 500 hPa in winter from 1980 to 2016. The latitude**  
 352 **and longitude coordinates of Beijing (green dot in base map) correspond to 40° N, 117° E,**  
 353 **respectively. The letters “L” and “H” in the base map demonstrate the near-surface**  
 354 **anomalous low- and high-pressure systems, respectively.**

355 We note a particular positive phase of SSTA series over the northwestern Pacific since the  
 356 mid-1980s. Consequently, an anomalously warm and high pressure or anti-cyclone system in the  
 357 mid-lower troposphere maintained over the region via air-sea interaction. This would in turn  
 358 induce anomalous southerly wind speeds from the near-surface to the mid-troposphere over the  
 359 East Asian continent, resulting in the weakening of the EAWM system. Particularly in the lower

360 troposphere, the weakening monsoons are more likely than before to be interrupted by persistent  
361 anomalous southerlies in North China, which facilitate the transportation of warm, moist air from  
362 the south to the north of eastern China, favorable for the occurrence of PHE in Beijing. In the  
363 mid-troposphere, a shallow East Asian trough also helps prevent cold-air activities from  
364 influencing Beijing, and is hence unfavorable for the clearance of pollutants around Beijing. These  
365 anomalous circulation patterns not only result in sinking air motion in the mid-lower troposphere,  
366 leading to a lower atmospheric boundary-layer height, which is unfavorable for vertical diffusion,  
367 but also give rise to stagnant weather conditions, and the collection of pollutants in the  
368 atmospheric boundary layer. Therefore, the increasing SST over the northwestern Pacific and the  
369 associated changes of atmospheric circulation related to a weakened EAWM system potentially  
370 play a key role in the increasing occurrences of weather conditions conducive to PHE in Beijing.  
371 So far we have discussed how the change of local pollution events in Beijing could be associated  
372 with large-scale climate warming via changes in EAWM and associated SSTA over the NW  
373 Pacific, as schematically depicted in Fig. 7.

374 Owing to its large heat capacity, the ocean accumulates energy derived from human activities,  
375 with more than 90% of the Earth's residual energy related to global warming absorbed by the  
376 ocean (IPCC, Cheng et al. 2017). As such, the record of the global ocean heat content robustly  
377 represents the signature of global warming, as it is less impacted by weather-related noise and  
378 climate variability such as El Niño and La Niña events (Cheng et al. 2018). The IPCC (2013) has  
379 concluded that it is very likely that anthropogenic forcings have made a substantial contribution to  
380 the increase of global upper ocean heat content (0–700 m) since the 1970s. It is worth to be  
381 mentioned that SST over the northwestern Pacific has been one of the most stable warming  
382 regions since the 20th century (Zeng et al., 2001). Based on the results of 15 models from the  
383 Coupled Model Intercomparison Project Phase 5 (CMIP5), Cai et al. (2017) projected some  
384 circulation changes induced by increasing atmospheric greenhouse gases likely contributing to the  
385 increase of haze events in Beijing. Our study presents a more concrete observation-based  
386 mechanism for explaining the extent to which climate change contributes to the increase of the  
387 occurrence of PHE in Beijing through changes in typical regional atmospheric circulation.

388 However, there are some caveats in the understanding of our results. In general, haze refers to an  
389 atmospheric phenomenon caused by fine particulate pollutants from various sources under specific  
390 meteorological conditions (Wang et al., 2013). The increased emissions of pollutants into the  
391 atmosphere because of the rapid development in China undoubtedly serve as the most important  
392 reason for increasing haze events in Beijing, as mentioned in many studies (e.g. Liu and Diamond,  
393 2005; Wang et al., 2013; Wang et al., 2014). Nevertheless, haze events in Beijing, especially PHE,  
394 have happened under specific persistent weather conditions, with our results revealing a novel  
395 perspective in relating local pollution changes in Beijing to large-scale climate change. Future  
396 work needs the quantification of the contributions of pollutant emissions and climate change to the  
397 occurrence of PHE in Beijing.

398 **Data availability.**

399 Atmospheric circulation data are available from the NCEP/NCAR data archive  
400 (<http://www.esrl.noaa.gov/psd/data/gridded/data.ncep.reanalysis.html>) and ECMWF data archive  
401 (<https://www.ecmwf.int/en/forecasts/datasets/browse-reanalysis-datasets>).

402 Sea-surface-temperature data are available from Met Office Hadley Centre observation datasets  
403 (<https://www.metoffice.gov.uk/hadobs/hadisst/>). The ground observations are from the National  
404 Meteorological Information Center of China (<http://data.cma.cn/>). The atmospheric composition  
405 data can be obtained from the authors.

406

407 **Competing interests:** The authors declare that they have no conflict of interest.

408 **Acknowledgements:** This study was supported by the National Key Research and Development  
409 Program of China (2016YFA0600404), the Beijing Natural Science Foundation (8161004), the  
410 Ministry of Science, Beijing Municipal Science and Technology Project (Z151100002115045),  
411 and the National Natural Science Foundation of China (41575010).

412

413 **References:**

414 Cai, W. J., Li, K., Liao, H., Wang, H. J. and Wu, L. X.: Weather conditions conducive to  
415 Beijing severe haze more frequent under climate change, *Nat. Clim. Change.*, 7(4),  
416 257-262, doi: 10.1038/NCLIMATE3249, 2017.

417 Chen, H. and Wang, H. J.: Haze days in north China and the associated atmospheric  
418 circulations based on daily visibility data from 1960 to 2012, *J. Geophys. Res-Atmos.*,  
419 120, 5895-5909, doi:10.1002/2015JD023225, 2015.

420 Cheng L. J., Trenberth, K., Fasullo, J., Boyer, T., Abraham, J., Zhu, J.: Improved estimates of  
421 ocean heat content from 1960 to 2015, *Science Advances*, 3, e16015452017, doi:  
422 10.1126/sciadv.1601545, 2017

423 Cheng, L. J., Trenberth, K. E., Fasullo, J., Abraham, J., Boyer, T. P., von Schuckmann, K., and  
424 Zhu, J.: Taking the pulse of the planet, *Earth and Space Science News, Eos.*, 99, 14-16,  
425 doi: 10.1029/2017EO081839, 2018.

426 Compo, G. P., Whitaker, J. S., Sardeshmukh, P. D., Matsui, N., Allan, R. J., Yin, X., Gleason, B.  
427 E., Vose, R. S., Rutledge, G., Bessemoulin, P., BroNnimann, S., Brunet, M., Crouthamel,



428 R. I., Grant, A. N., Groisman, P. Y., Jones, P. D., Kruk, M. C., Kruger, A. C., Marshall, G.  
429 J., Maugeri, M., Mok, H. Y., Nordli, O., Ross, T. F., Trigo, R. M., Wang, X. L., Woodruff,  
430 S. D., and Worley, S. J.: The twentieth century reanalysis project, *Q. J. Roy. Meteor. Soc.*,  
431 137(654), 1-28, doi: 10.1002/qj.776, 2011.

432 Ding, Y. H. and Liu, Y. J.: Analysis of long-term variations of fog and haze in China in recent  
433 50 years and their relations with atmospheric humidity, *Sci. China. Earth. Sci.*, 57, 36-46,  
434 doi: 10.1007/s11430-013-4792-1, 2014.

435 Doyle, M., and Dorling, S.: Visibility trends in the UK 1950–1997, *Atmos. Environ.*, 36,  
436 3161-3172, doi: 10.1016/j.atmosres.2009.05.006, 2002.

437 Gao, M, Guttikunda, S. K., Carmichael, G. R., Wang, Y., Liu, Z., Stanier, C. O., Saide, P. E.  
438 and Yu, M.: Health impacts and economic losses assessment of the 2013 severe haze  
439 event in Beijing area, *Sci. Total. Environ.*, 511: 553-561, doi:  
440 10.1016/j.scitotenv.2015.01.005, 2015.

441 Guo, J. P, Zhang, X. Y., Wu, Y. R, Zhaxi, Y. Z., Che, H. Z, La, B., Wang, W. and Li, X. W:  
442 Spatiotemporal variation trends of satellite-based aerosol optical depth in China during  
443 1980-2008, *Atmos. Environ.*, 45, 6802-6811. doi:10.1016/j.atmosenv.2011.03.068, 2011.

444 He, H., Wang, X. M, Wang, Y. S, Wang, Z. F, Liu, J. G. and Chen, Y. F.: Formation mechanism  
445 and control strategies of haze in China, *Bull. Chinese. Acad. Sci.*, 28 (3), 344-352, doi:  
446 10.3969/j.issn.1000-3045.2013.03.008, 2013.

447 Hou, Q., An, X. Q., Wang, Y., Tao, Y. and Sun, Z. B.: An Assessment of China's PM<sub>10</sub>-related  
448 Health Economic Losses in 2009, *Sci. Total. Environ.*, 435-436:61-65,  
449 doi:org/10.1016/j.scitotenv.2012.06.094, 2012.

450 Huang, N. E., Shen, Z., Long, S. R., Wu, M. C., Shih, H. H., Zheng, Q., Yen, N. C., Tung, C.  
451 C. and Liu, H. H.: The empirical mode decomposition and the Hilbert spectrum for  
452 nonlinear and nonstationary time series analysis, *Proc. Roy. Soc. London. Series. A.*,  
453 454:903–995, doi: 10.1098/rspa.1998.0193, 1998.

454 Huang, N. E., Wu, Z. H.: A review on Hilbert-Huang transform: method and its applications to  
455 geophysical studies, *Rev. Geophys.*, 46:RG2006, doi:10.1029/2007RG000228, 2008.

456 Huang, R. J., Zhang, Y. L., Bozzetti, C., Ho, K. F., Cao, J. J., Han, Y. M., Deallanbach, K. R.,  
457 Slowik, J. G., Platt, S. M., Canonaco, F., Zotter, P., Wolf, R., Pieber, S. M., Bruns, E. A.,

458 Crippa, M., Ciarelli, G., Piazzalunga, A., Schwikowski, M., Abbaszade, G.,  
459 Schnelle-Kreis, J., Zimmermann, R., An, Z., Szidat, S., Baltensperger, U., Haddad, I. E.  
460 and Prevot, A.S.H.: High secondary aerosol contribution to particulate pollution during  
461 haze events in China, *Nature*, 514, 218-222, doi: 10.1038/nature13774, 2014.

462 Huang, R. H., Chen, J. L., Wang, L. and Lin, Z. D.: Characteristics, processes, and causes of  
463 the spatio-temporal variabilities of the East Asian monsoon system, *Adv. Atmos. Sci.*,  
464 29(5):910-942, doi.org/10.1007/s00376-013-0001-6, 2012.

465 IPCC: Climate Change 2013: The Physical Science Basis. Contribution of Working Group I to  
466 the Fifth Assessment Report of the Intergovernmental Panel on Climate Change, 2013.

467 Kalnay, E., Kanamitsu, M., Kistler, R., Collins, W., Deaven, D., Gandin, L., Iredell, M., Saha,  
468 S., White, G., Woollen, J., Zhu, Y., Leetmaa, A., Reynolds, B., Chelliah, M., Ebisuzaki,  
469 W., Higgins, W., Janowiak, J., Mo, K. C., Ropelewski, C., Wang, J., Jenne, R., Joseph, D.:  
470 The NCEP/NCAR 40-year reanalysis project, *Bull. Amer. Meteor. Soc.*, 77, 437-470,  
471 doi:10.1175/1520-0477(1996)077<0437:TNYRP>2.0.CO;2, 1996.

472 Li, Q., Zhang, R. H. and Wang, Y.: Interannual variation of the wintertime foghaze days across  
473 central and eastern China and its relation with East Asian winter monsoon, *Int. J.*  
474 *Climatol.*, 36, 346-354, doi: 10.1002/joc.4350, 2016.

475 Liao, X. N., Zhang, X. L., Wang, Y. C., Liu, W. D., Du, J. and Zhao, L. H.: Comparative  
476 analysis on meteorological condition for persistent haze cases in Summer and Winter in  
477 Beijing, *Environ. Sci.*, 35(6):2031-2044, (in Chinese), doi:10.13227/j.hjcx.2014.06.001,  
478 2014.

479 Liu, J. and Diamond, J.: China's environment in a globalizing world, *Nature*, 435, 1179-1186.  
480 doi: 10.1038/4351179a, 2005.

481 Niu, F., Li, Z. Q., Li, C., Lee, K. H. and Wang, M. Y.: Increase of wintertime fog in China:  
482 potential impacts of weakening of the eastern Asian monsoon circulation and increasing  
483 aerosol loading, *J. Geophys. Res.*, 115, D00K20, doi: 10.1029/2009JD013484, 2010.

484 Poli, P., Hersbach, H., Dee, D. P., Berrisford, P., Simmons, A. J., Vitart, F., Laloyaux, P., Tan,  
485 D. G. H., Peubey, C., Thepaut, J. N., Tremolet, Y., Holm, E. V., Bonavita, M., Isaksen, L.  
486 and Fisher, M.: ERA-20C: An atmospheric reanalysis of the 20th century, *J.Clim.*,  
487 29(11):4083-4097, doi: 10.1175/JCLI-D-15-0556.1, 2016.

488 Pope, C. A. III., and Dockery, D. W.: Health effects of fine particulate air pollution: Lines that  
489 connect, *J. Air. Waste. Manage. Assoc.*, 56(6), 709-742,  
490 doi:10.1080/10473289.2006.10464484, 2006.

491 Qian, C., Fu, Z. B., Zhou, T. J.: On multi-timescale variability of temperature in China in  
492 modulated annual cycle reference frame, *Adv. Atmos. Sci.*, 27(5), 1169-1182. doi:  
493 10.1007/s00376-009-9121-4, 2010.

494 Rayner, N. A., Parker, D. E., Horton, E. B., Folland, C. K., Alexander, L., Rowell, D. P., Kent,  
495 E. and Kaplan, A.: Global analyses of sea surface temperature, sea ice, and night marine  
496 air temperature since the late nineteenth century, *J. Geophys. Res-Atmos.*, 108  
497 (D14):1063-1082. doi: 10.1029/2002JD002670, 2003.

498 Schichtel, B. A., Husar, R. B., Falke, S. R., and Wilson, W. E.: Haze trends over the United  
499 States 1980–1995, *Atmos. Environ.*, 35, 5205–5210, doi:  
500 10.1016/S1352-2310(01)00317-X, 2001.

501 Sun, J. Q., Wu, S. and Ao, J.: Role of the North Pacific sea surface temperature in the East  
502 Asian winter monsoon decadal variability, *Clim. Dyn.*, 46(11-12): 3793-3805, doi:  
503 10.1007/s00382-015-2805-9, 2016.

504 Sun, Y. L., Jiang, Q., Wang, Z. F., Fu, P. Q., Li, J., Yang, T. and Yin, Y.: Investigation of the  
505 sources and evolution processes of severe haze pollution in Beijing in January 2013, *J.*  
506 *Geophys. Res-Atmos.*, 119(7): 4380-4398, doi: 10.1002/2014JD021641, 2014.

507 Sun, Z., An, X. Q., Yan, T. and Hou, Q.: Assessment of population exposure to PM10 for  
508 respiratory disease in Lanzhou (China) and its health-related economic costs based on  
509 GIS, *Bmc. Public. Health.*, 13(1):1-9, doi: 10.1186/1471-2458-13-891, 2013.

510 Tang, G., Zhu, X., Hu, B., Xin, J., Wang, L., Munkel, C., Mao, G. and Wang, Y.: Impact of  
511 emission controls on air quality in Beijing during APEC 2014: lidar ceilometer  
512 observations, *Atmos. Chem. Phys.*, 15(21):12667-12680, doi:  
513 10.5194/acp-15-12667-2015, 2015.

514 Vautard, R., Yiou, P., and Oldenborgh, G.: Decline of fog, mist and haze in Europe over the  
515 past 30 years, *Nat. Geosci.*, 2, 115-119, doi:10.1038/NGEO414, 2009.

516 Wang, H. J., Chen, H. P. and Liu, J.: Arctic sea ice decline intensified haze pollution in eastern  
517 China, *Atmos. Ocean. Sci. Lett.*, 8, 19, doi: 10.3878/AOSL2014081, 2015.

518 Wang, H. J. and He, S. P.: The increase of snowfall in northeast China after the mid-1980s,  
519 Chin. Sci. Bull., 58(12), 1350-1354, 2013.

520 Wang, L. T., Wei, Z., Yang, J., Zhang, Y., Zhang, F. F., Su, J., Meng, C. C. and Zhang, Q.: The  
521 2013 severe haze over southern Hebei, China: model evaluation, source apportionment,  
522 and policy implications, Atmos. Chem. Phys., 14(6): 3151-3173, 2014.

523 Wang, X. P., and Mauzerall, D. L.: Evaluating impacts of air pollution in China on public  
524 health: Implications for future air pollution and energy policies, Atmos. Environ., 40(9),  
525 1706–1721, doi: 10.1016/j.atmosenv.2005.10.066, 2006.

526 Wang, Y. S., Zhang, J. K., Wang, L. L., Hu, B., Tang, G. Q., Liu, Z. R., Sun, Y., and Ji, D. S.:  
527 Researching significance, status and expectation of haze in Beijing-Tianjin-Hebei region,  
528 Advances in Earth Science, 29(3), 388–396, (in Chinese), doi:  
529 10.5194/acpd-13-28395-2013, 2014.

530 Wang, Y. S., Yao, L., Liu, Z. R., Ji, D. S., Wang, L.L, and Zhang, J. K.: Formation of haze  
531 pollution in Beijing—Tianjin—Hebei region and their control strategies, Bull. Chinese  
532 Acad. Sci., 28(3)353-363, 2013.

533 World Meteorological Organization (WMO): Guide of Meteorological Instruments and  
534 Methods of Observation, Eos Transactions, 55, 2008.

535 World Meteorological Organization: The First WMO Intercomparison of visibility  
536 Measurement: Final Report (D. J. Griggs, D. W. Jones M. Ouldrige, W. R. Sparks)  
537 Instrument and Observing Methods Report No. 41, WMO/TD.401, Geneva, 1990.

538 Wu, D.: More discussions on the differences between haze and fog in city, Guangdong  
539 Meteorology, 32, 9–15, (in Chinese), 2006.

540 Wu, P., Ding, Y. H. and Liu, Y. J.: Atmospheric Circulation and Dynamic Mechanism for  
541 Persistent Haze Events in the Beijing–Tianjin–Hebei Region, Adv.Atmos.Sci.,  
542 34(4):429-440, doi: 10.1007/s00376-016-6158-z, 2017.

543 Wu, Z., Huang, N. E., Long, S. R., Peng, C. K.: On the trend, detrending, and variability of  
544 nonlinear and nonstationary time series, Proc.Natl.Acad.Sci. U.S.A.,  
545 104(38):14889-14894, doi:10.1073/pnas.0701020104, 2007.

546 Wu, Z., Huang, N. E.: Ensemble empirical mode decomposition: a noise-assisted data analysis  
547 method, Adv. Adapt. Data. Anal., 1:1-41, doi:10.1142/S1793536909000047, 2009.

548 Wu, D., Wu, X., Zhu, X.: Fog and Haze in China. China Meteorological Press: Beijing, 37-59,  
549 (in Chinese), 2009.

550 Wu, D., Chen, H. Z, Wu, M., Liao, B. T., Wang, Y. C., Liao, X. N., Zhang, X. L., Quan, J. N.,  
551 Liu, W. D., Gu, Y., Zhao, X. J., Meng, J. P., Sun, D.: Comparison of three statistical  
552 methods on calculating haze days-taking areas around the capital for example, China  
553 Environmental Science, 34(3), 545-554, (in Chinese), 2014.

554 Xie, Y. B., Chen, J., and Li, W.: An assessment of PM<sub>2.5</sub> related health risks and impaired  
555 values of Beijing residents in a consecutive high-level exposure during heavy haze days,  
556 Environ. Sci., 35(1), 1-8, (in Chinese), 2014.

557 Xu, P., Chen, Y. F., and Ye, X. J.: Haze, air pollution, and health in China. Lancet, 382, 2067,  
558 doi:10.1016/S0140-6736(13)62693-8, 2013.

559 Yin, Z. C. and Wang, H. J.: The relationship between the subtropical Western Pacific SST and  
560 haze over North-Central North China Plain, Int. J. Climatol., 36(10):3479-3491, doi:  
561 0.1002/joc.4570, 2016.

562 Yin, Z. C. and Wang, H. J.: Role of atmospheric circulations in haze pollution in December  
563 2016, Atmos. Chem. Phys., 17(18):1-21. doi: 10.5194/acp-17-11673-2017, 2017.

564 Zeng, Z. M., Yan, Z. W. and Ye, D. Z.: Regions of most significant temperature trend during  
565 the last century, Adv. Atmos. Sci., 18(4):481-496, doi: 10.1007/s00376-001-0039-8,  
566 2001.

567 Zhang, L., Wang, T., Lv, M. and Zhang, Q.: On the severe haze in Beijing during January  
568 2013: Unraveling the effects of meteorological anomalies with WRF-Chem, Atmos.  
569 Environ., 104: 11-21, doi: 10.1016/j.atmosenv.2015.01.001, 2015.

570 Zhang, R., Jing, J., Tao, J., Hsu, S. C., Wang, G., Cao, J., Lee, C. S. L, Zhu, L., Chen, Z., Zhao,  
571 Y. and Shen, Z.: Chemical characterization and source apportionment of PM<sub>2.5</sub> in  
572 Beijing: seasonal perspective, Atmos. Chem. Phys., 13, 70537074, doi:  
573 doi:10.5194/acp-13-7053-2013, 2013.

574 Zhang, R. H., Li, Q., and Zhang, R. N.: Meteorological conditions for the persistent severe fog  
575 and haze event over eastern China in January 2013, Sci. China. Earth. Sci., 57, 26-35,  
576 doi: 10.1007/s11430-013-4774-32014, 2013.

577 Zhang, Y. J., Zhang, P. Q., Wang, J., Qu, E. S, Liu, Q. F. and Li, G.: Climatic characteristics of

578 persistent haze event over Jingjinji during 1981-2013, *Meteorology*, 41(3), 311-318, (in  
579 Chinese), doi: 10.7519/j.issn.1000-0526.2013.03.006, 2014.

580 Zhou, Y., Wu, Y. and Yang, L.: The impact of transportation control measures on emission  
581 reductions during the 2008 Olympic Games in Beijing., China. *Atmos. Environ.*, 44,  
582 285-293, doi: 10.1016/j.atmosenv.2009.10.040, 2010.

583 Zhu, X., Tang, G., Hu, B., Wang, L., Xin, J., Zhang, J., Liu, Z., Munkel, C., and Wang, Y.:  
584 Regional pollution characteristics and formation mechanism over Beijing-Tianjin-Hebei  
585 area: a case study with model simulation and ceilometers observation, *J. Geophys.*  
586 *Res-Atmos.*, 121, doi: 10.1002/2016JD025730, 2016.

587 Zou, Y. F., Wang, Y. H., Zhang, Y. H. and Koo, J. H.: Arctic sea ice, Eurasia snow, and  
588 extreme winter haze in China, *Science Advances*, 3(3):e1602751, doi:  
589 10.1126/sciadv.1602751, 2017.

590

591

592